

precipitation intensity, the frequency distribution of precipitation rates, and minimum detectable rain rate.

2 Data sets

The TRMM satellite data sets are processed to yield several types of relative error statistics in this study. We also examined the plausibility of the TRMM products compared to existing empirical knowledge. TMI and PR instantaneous rain rates are compared over ocean and land using orbit data from V6 TRMM products 2A-12, representing the TMI rainfall retrieval, and 2A-25, representing the PR rainfall retrieval.

Within the TMI instantaneous algorithm 2A-12, 85 GHz and 19 GHz are the heaviest weighted channels over ocean and land, respectively (Kummerow et al. 1996). We use the “near surface” values for rain rates, which are available in both V5 and V6 products.

3 TMI regional probability density functions (PDFs) of rain rate

The global ocean PDF is a superposition of the regional ocean PDFs. A closer look at oceanic geographic regions $\sim 2.25 \times 10^6 \text{ km}^2$ in scale over 47-day periods showed that the degree of agreement between PR and TMI PDFs varies regionally. Some oceanic regional PDFs have become less plausible in V6 than in V5. Notably, several regional PDFs for TMI V6 ocean have a physically implausible bimodal structure (Fig. 1). The corresponding PR V5 and PR V6 PDFs are unimodal. Many regions with heavy tropical

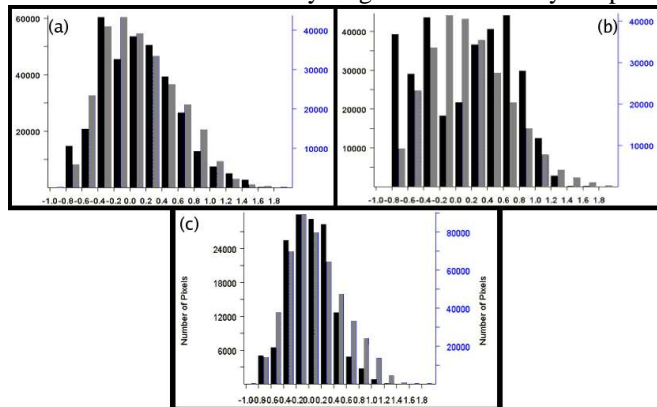


Fig. 1. Overlaid PDFs for TRMM V5 and V6 regional oceanic rain rates. Rain rates from PR are in grey and from the TMI swath overlapping PR are in black. PDFs represent accumulated statistics of instantaneous rain rates for 47 days of orbit products from 16 June – 1 August 2001 (pre-boost). (a) V5 Tropical Western Pacific near Kwajalein. (b) V6 Tropical Western Pacific near Kwajalein. (c) V6 Southwest Pacific between Australia and New Zealand.

precipitation during the summer season, such as the tropical western Pacific near Kwajalein, show problematic PDFs in V6 TMI (Fig. 1b) that are not present in V5 (Fig. 1a). Some PDFs at higher latitudes also exhibit bimodal characteristics, such as the western Atlantic off the US coast. Other PDFs have the expected unimodal characteristics, such as the southwest Pacific between the east coast of Australia and New Zealand during the local winter (Fig. 1c). Figure 2 shows the geographic distribution of the various PDF modes in June and January. The bimodal PDFs occur more often in local summer months.

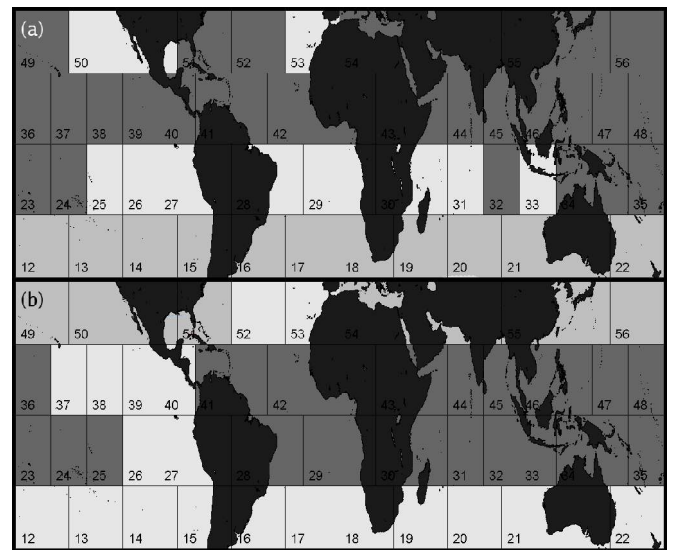


Fig. 2. Map of oceanic regional PDF shape for 47 day accumulated V6 TMI instantaneous rain rates. Color coding indicates unimodal (medium grey), bimodal (dark grey), and strongly skewed (light grey) distributions in $\log_{10}(R)$. (a) Northern Hemisphere (NH) summer from 16 June – 1 August 2001. (b) NH winter from 1 Jan – 16 Feb 2002. Grid numbers are in lower left corner of each grid box.

4 TMI spatial discontinuities

Over the ocean, both scattering and emission channels are used to derive the rain rate. Over the land and coast, the satellite-observed emission from precipitation is contaminated by emissions from the surface. Because the emission signal from heavy rainfall over land cannot be readily distinguished from radiation emitted from the land surface, the rainfall retrieval algorithms for the TMI must rely heavily on the scattering signal from ice. As a result, the emission channels are not weighted heavily over land and are not used at all over coast (Kummerow et al. 1996). The different sets of information available to the precipitation retrieval algorithms for land and coast versus ocean can lead to discontinuities in the retrieved precipitation field.

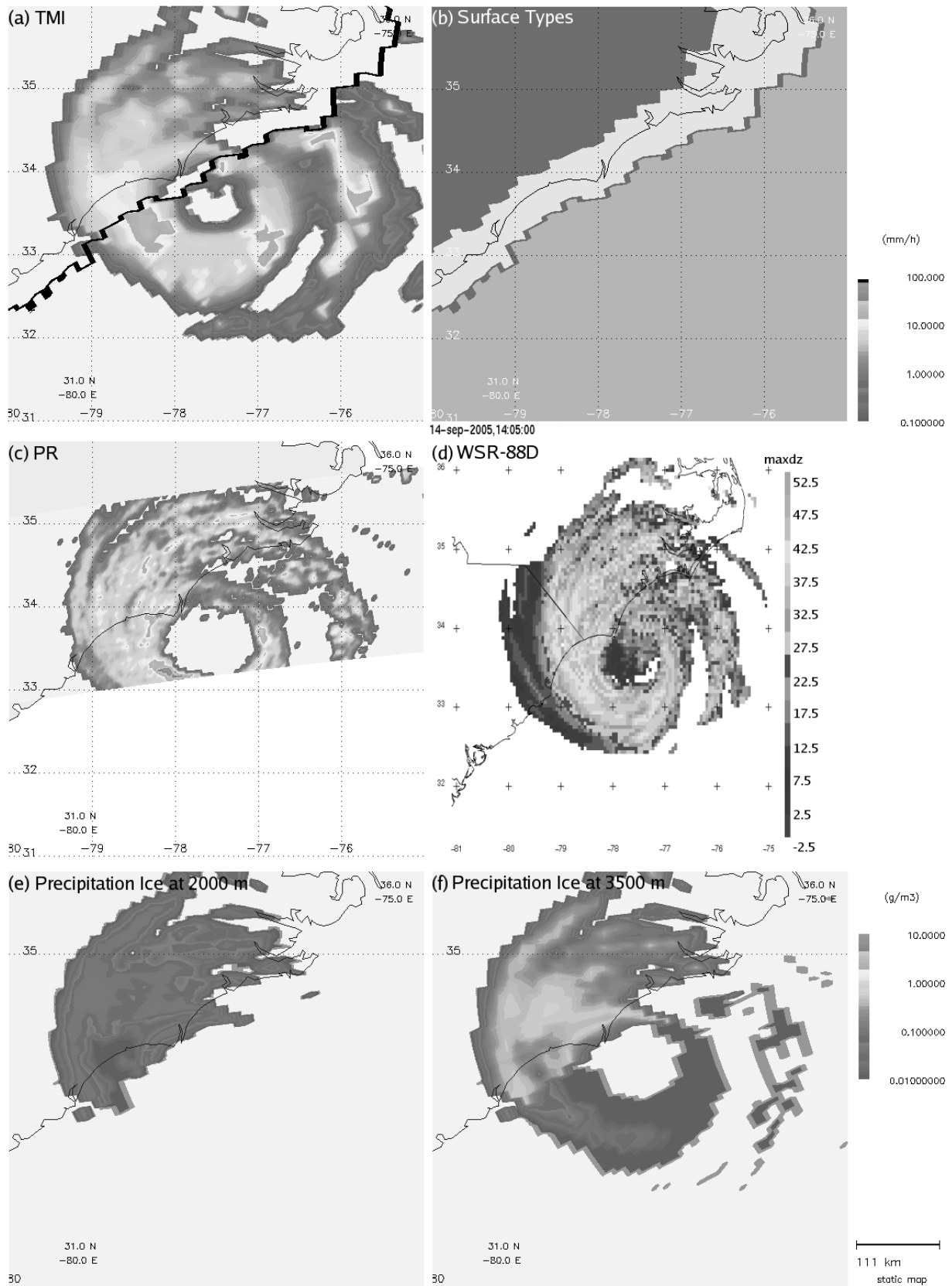


Fig. 3. Views from different sensors of Hurricane Ophelia straddling the North Carolina coast at ~1400 UTC on 14 September 2005. (a) TMI precipitation retrieval with coast/ocean surface border overlaid. (b) Surface masked used in 2A-12: land, coast, and ocean. (c) PR near surface precipitation. (d) Combined radar reflectivity from coastal NWS WSR-88D radars at Morehead City, NC and Wilmington, NC. (e) TMI precipitation ice at 2000 m about the surface. (f) TRMM 2A-25 precipitation ice at 3500 m above the surface.

The TMI precipitation retrieval algorithm over the ocean differs from that over the land and coast (McCollum and Ferraro 2003). Figure 3 compares the precipitation retrieval from the TRMM PR and the TMI for Hurricane Ophelia over the North Carolina coast. The TMI retrieved rain rate field has abrupt discontinuities along the boundaries between ocean and coast (Fig. 3a). These discontinuities are not observed in either the TRMM PR derived rain rates or the near-surface reflectivity obtained by National Weather Service (NWS) WSR-88D radar. In the Ophelia case, the limited information from the 85.5 GHz channel leads to an underestimation of rainfall rates over land surfaces and spatial errors when locating areas of intense rainfall. The size and shape of the eye of the hurricane in the TMI rain field is also inconsistent with the PR and NEXRAD observations. Disagreement between the TMI and PR indicates observational and processing errors in one or both instruments. These inconsistencies lead to errors in the data and analyses that are derived from the TRMM observations.

Within the TMI 2A-12 algorithm, vertical profiles of hydrometeors are associated with the observed TMI brightness temperatures and estimated surface rain rates. Profiles of cloud liquid water, precipitation liquid water, cloud ice, and precipitation ice are included as part of the 2A-12 product. The hydrometeor profiles provide a valuable diagnostic of an intermediate step within the TMI algorithm.

For the Ophelia case, the freezing level is at ~ 4500 m altitude. Alarming, precipitation ice is present at altitudes below the freezing level in the TMI product over both land and ocean (Fig. 3e/f). Preliminary investigation of several storms has shown that the TMI algorithm often yields erroneous precipitation ice within rain layers at altitudes well below the freezing level. The non-physical presence of ice below the freezing level is an indication of a serious error in the TMI algorithm physics.

5 Conclusions

Analysis of relative errors between TMI and PR V5 and V6 data sets reveals some steps forward and backward in the TRMM algorithms. Relative differences were examined in regional and instantaneous orbit data sets. TMI and PR were compared to each other and NWS radar to identify relative errors in the TRMM observations.

Examination showed that approximately half of the regional PDFs of V6 TMI oceanic rain rate exhibit an implausible bimodal distribution of rain rates that is not present in either PR V6 or V5 products. These implausible bimodal

characteristics in TMI oceanic rain rate PDFs are present in a subset of the oceanic tropical and midlatitude regions, most commonly during the local summer.

Comparison of TMI and PR data for several coastal precipitation events shows that there can be serious problems with TMI rainfall estimations at the ocean-coast boundary. The TMI had a physically implausible rain rate field that was discontinuous along the surface type boundaries between coast and ocean where the algorithm transitions from using all channels to just 85.5 GHz (Fig. 3). The presence of this discontinuity along the surface type boundary signals a problem with the TMI precipitation retrieval algorithm in the cases examined. Additionally, the spurious presence of precipitation ice in the lowest levels of the TMI profile below the freezing layer is another symptom of error in the V6 TMI precipitation algorithm.

To be useful to the wider community, TRMM satellite precipitation retrievals must yield the right answers for the right reasons. Several types of relative error characteristics have improved between V5 and V6. However, changes to the TMI oceanic precipitation algorithm from V5 to V6 appear to have had unintended side effects that have degraded some regional TMI oceanic precipitation retrievals. The location and intensity of precipitation within these regions is such that these degradations are significant to global precipitation. The problems observed in the oceanic and coastal regions need further investigation, diagnosis, and correction.

Acknowledgments: This work was funded by National Aeronautics and Space Administration grants NNG04GA65G and NNG04GF33A.

References

- Kummerow, C., W. S. Olson, and L. Giglio, 1996: A simplified scheme for obtaining precipitation and vertical hydrometeor profiles from passive microwave sensors. *IEEE Trans. Geosci. Remote Sens.*, **34**, 1213-1232.
- Kummerow, C., W. Barnes, T. Kozu, J. Shue, and J. Simpson, 1998: The Tropical Rainfall Measuring Mission (TRMM) sensor package. *J. Atmos. Ocean. Tech.*, **15**, 809-817.
- McCollum, J. R., and R. R. Ferraro, 2003: Next generation of NOAA/NESDIS TMI, SSM/I, and AMSR-E microwave land rainfall algorithms. *J. Geophys. Res.*, **108**, doi: 10.1029/2001JD001512.